Tetrahedron 67 (2011) 3412–3419

Contents lists available at ScienceDirect

Tetrahedron

journal homepage: www.elsevier.com/locate/tet

Ratiometric fluorescent Zn^{2+} chemosensor constructed by appending a pair of carboxamidoquinoline on 1,2-diaminocyclohexane scaffold

Xiaobo Zhou [a], Yunguo Lu [a], Jian-Fa Zhu [a], Wing-Hong Chan [a,*], Albert W.M. Lee [a], Pui-Shan Chan [b], Ricky N.S. Wong [b], N.K. Mak [b]

[a] Department of Chemistry, Hong Kong Baptist University, Hong Kong, China
[b] Department of Biology, Hong Kong Baptist University, Hong Kong, China

ARTICLE INFO

Article history:
Received 16 December 2010
Received in revised form 8 March 2011
Accepted 17 March 2011
Available online 25 March 2011

Keywords:
Zinc chemosensor
Fluorescence
Ratiometric
Molecular switch
Cell imaging

ABSTRACT

By appending a pair of carboxamidoquinoline pendants onto 1,2-diaminocyclohexane scaffold via *N*-alkylation, multifunctionalized **ACAQ** was designed and synthesized as a water soluble fluorescent ratiometric chemosensor for Zn^{2+}. In 50% aqueous methanol buffer pH 7.4 solution, upon excitation at 316 nm, **ACAQ** (5 μM) displayed a selective ratiometric fluorescence changes with a shift from 410 to 490 nm in response to the interaction with Zn^{2+}. After binding with 1 equiv of Zn^{2+}, **ACAQ** exhibited a 12-fold enhancement in I_{490}/I_{410} characterized by a clear isoemissive point at 440 nm. The metal sensor binding mode was established by Job's plot and the combined fluorescence and ^1H NMR spectroscopic method. The selectivity of the probe toward biological relevant cations and transition metal ions was proven to be good. In addition, the interference caused by Cu^{2+} and Cd^{2+} in the quantitation of Zn^{2+} can be completely eliminated by the use of diethyldithiocarbamate as the screening agent. Exploitation of **ACAQ** as the sensing probe, ratiometric determination of Zn^{2+} with the limit of detection (LOD) at 28.3 nm can be realized. In addition, the unique responsive properties of the probe toward Fe^{3+} and Zn^{2+} were used to construct a fluorescent switch. The membrane permeability of **ACAQ** to living cells and bio-imaging of Zn^{2+} were demonstrated.

1. Introduction

The design and synthesis of metal chemosensors with high selectivity and sensitivity is an active field in supramolecular chemistry.[1] Particular attention has been focused on targeting heavy and/or transition metal (HTM) ions, for their detection in the cell environment.[2] Zinc(II) ion is the second most abundant transition metal essential for the human body with a concentration ranging from sub-nm to 0.3 mM.[3] The detection and imaging of Zn^{2+} in biological samples are of significant interest owing to its unique role in physiological functions.[4] Numerous scientific endeavors have been engaged in the development of fluorescent chemosensors for the in vitro and in vivo detection of Zn^{2+}.[5] For instance, Yoon's group has recently reported a highly selective, cell-permeable, and ratiometric fluorescent sensor for Zn^{2+}.[6] However, some of the reported Zn^{2+} sensors have poor water solubility and are vulnerable to the interference by other metal ions.[5e–g] Furthermore, the majority of existing sensors may not be able to perform the sensing in cell environment.[5d,g], Therefore, the development of a more versatile and improved performance fluorescent sensors is still in great demand.

In response to such challenge, we have continued our quest for novel fluorescence metal chemosensor development, especially targeting at Zinc metal.[7] To be of practical value in real sample determination including in vivo cell imaging, the probe preferably possesses the following attributes: (1) it should be readily accessible from a reliable synthetic route; (2) it should be operative in aqueous buffer pH 7.4 solution; (3) it must be a sensitive and selective probe; (4) among all signal transduction mechanism, it should follow either fluorescence turn-on or ratiometric mode of response. From this background, to sustain our interests in the sensor development, herein, we present a new fluorescent ratiometric chemosensor **ACAQ** capable of responding sensitively and selectively to zinc ion in aqueous buffer pH 7.4 solutions.

2. Results and discussion

On the basis of the prevalent fluorescence sensors design protocol, we call for the construction of 'fluorophore-spacer-receptor-spacer-fluorophore' sensor motif as shown in Scheme 1.[8] To confer the synthetic host with selective binding affinity to transition metal

* Corresponding author. Tel.: +852 3411 7076; fax: +852 3411 7348; e-mail address: whchan@hkbu.edu.hk (W.-H. Chan).

0040-4020/$ – see front matter © 2011 Elsevier Ltd. All rights reserved.
doi:10.1016/j.tet.2011.03.053

ions, fluorophores with metal binding ability are tethered with a semi-rigid multifunctional receptive molecular platform. Taking advantage of its high fluorescence quantum yield and metal binding capability, bidentate 8-carboxamidoquinoline moiety was chosen as the functional fluorophore for metal sensor development.[5a,f,g,9] To maximize the binding sites of the sensor intending to accommodate six-coordinated zinc metal, *trans*-1,2-diaminocyclohexane was selected and allowed to conjugate with a pair of functionalized 8-carboxamidoquinoline affording sensor **ACAQ** via a short synthetic route as depicted in Scheme 2. On the outset of the investigation, we recognize the fact that to be a viable probe operative in aqueous medium, the binding energy of the probe and the metal ion must be comparable to that of the hydration energy of the metal ion. Guided by this principle, we first utilize the vicinal diamino group of 1,2-diaminocyclohexane acting as strong ligands for transition metals to construct the metal sensing scaffold. This will be followed by incorporating two side-armed 8-aminoquinoline derived pendants to furnish sensor **ACAQ**. It is noteworthy that the two pendants can provide four additional cooperative ligating sites (i.e., two quinolyl nitrogens and two amido moieties) so as to endow the sensor with a maximum of six coordinating ligands. Implementation of the rational sensor design mentioned above, treatment of 8-aminoquinoline with 2-bromoacetyl bromide in the presence of triethylamine gave the corresponding amide **1** in 96% yield.[7b] One extra-step by *N*-alkylating on 1,2-diaminocyclohexane with 2 equiv of **1** in the presence of triethylamine enabled us to obtain the target **ACAQ** in 61% chemical yield. The structure and the purity of **ACAQ** were adequately confirmed by ^{1}H, ^{13}C NMR and HRMS analysis.

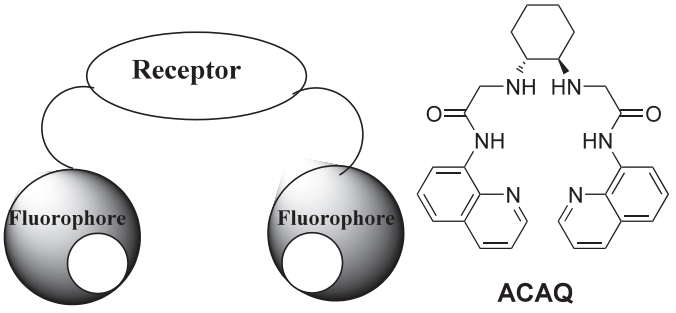

Scheme 1. 'Fluorophore-spacer-receptor-spacer-fluorophore' sensor design.

As shown in Fig. 1, upon addition of up to 1 equiv of Zn^{2+} in 50% aqueous methanol buffer solution of **ACAQ**, the absorbance at 237 and 315 nm decreased with concomitant formation of new peaks at 250 and 350 nm, resulting in the formation of a light yellow solution at the end of the titration. Clear isosbestic points at 280 and 326 nm were apparent, which indicates the formation of only one active zinc complex with the probe. Furthermore, a linear dependence of the absorbance at 350 nm as a function of Zn^{2+} concentration was observed (inset, Fig. 1). Among all other transition metals, only Cd^{2+} and Cu^{2+} can give similar results in their respective UV–vis titration curve with **ACAQ** (Figs. S1 and S2, Supplementary data). On the basis of non-linear fitting of the titration curve of 1:1 binding model (vide infra), the association constant of Zn^{2+}–**ACAQ**, Cu^{2+}–**ACAQ** and Cd^{2+}–**ACAQ** were computed to be 1.84×10^{6}, 1.92×10^{6} and 3.20×10^{6} M^{-1}, respectively.

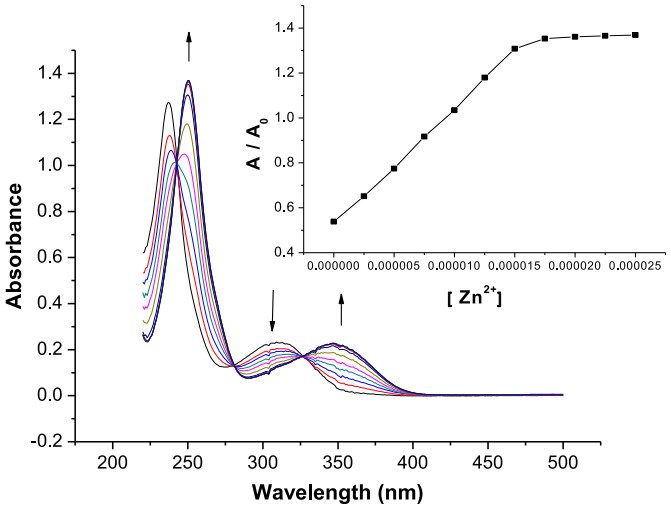

Fig. 1. UV–vis spectra of **ACAQ** (10 μM) upon the titration of Zn^{2+} (0–1 equiv) in buffer solution (50 mM HEPES, 50% methanol, pH=7.4). Inset: calibration curve in which $A_{250\ nm}$ as a function of Zn^{2+} concentration.

Due to the intrinsic high sensitivity associated with fluorescent detection, fluorescent sensors, particularly turn-on or ratiometric sensors, are desirable and very much sought after sensing devices. Fluorescence titration of **ACAQ** toward Zn^{2+} revealed that **ACAQ** can be developed as a ratiometric sensor for Zn^{2+} (Fig. 2). Upon gradual addition of Zn^{2+} into 5 μM **ACAQ** measuring solution, with

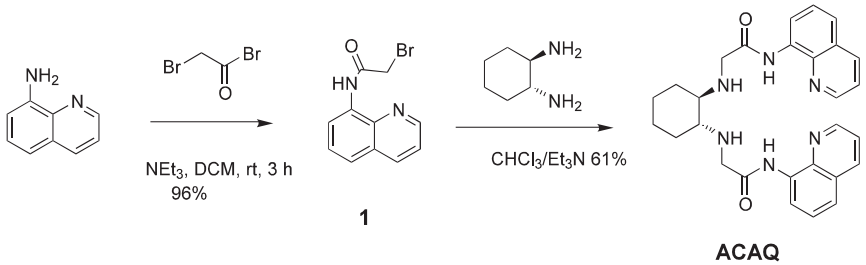

Scheme 2. Facile synthesis of **ACAQ**.

To test the viability of using **ACAQ** as a Zn^{2+} sensor, we first performed the UV–vis titration of the sensor with Zn^{2+} ion. To attain real analytical application value, chemosensing of metal ions should preferably be performed in aqueous conditions. To confer the sensory system with the potential for cell imaging, the sensing process will be examined in buffer pH 7.4 solutions. To this end, encouraged by some preliminary results, the sensing of Zn^{2+} in fact can be carried out in 50% aqueous methanol HEPES buffer solutions. λ_{ex}=316 nm, the emission peak of the sensor at 410 nm decreased with concomitant formation of a new peak at 490 nm. On further addition of Zn^{2+} into the probe, the ratiometric change of the fluorescence spectra became evident with a clear isoemission point at 430 nm. The emission ratio of I_{490}/I_{410} remained at a plateau in the presence of an excess of Zn^{2+} (inset, Fig. 2). Additionally, the observed 70 nm bathochromatic shift of the probe after binding with Zn^{2+} is conceivably triggered by Intramolecular Charge

Transfer (ICT).[10] It is noteworthy that ICT sensors exhibiting both intensity changes and spectral shifts are ideal molecular platforms to design ratiometric sensors. More concrete support of the response mechanism of the probe will be provided by ^{1}H NMR spectral method (vide infra). The ratio of I_{490}/I_{410} recorded an enhancement of 12-fold from 0.5 for bare sensor to 6.0 for 1:1 metal–sensor complex. The limit of detection (LOD) estimated from seven repeated measurements for Zn^{2+} detection is 28.3 nm. On the other hand, the fluorescence of the probe and the Zn^{2+}–probe increased slightly from pH 4.0 to 6.0, reached a plateau of a stable reading from pH 6.0 to 10.0, covering the physiological pH window (Fig. S3, Supplementary data). Presumably, under acidic conditions, protonation at the quinolyl nitrogen of the probe on one hand weakens its interaction with the metal and on the other hand slightly enhances the fluorescence of the probe. Therefore, subsequent metal binding studies were carried out in HEPES buffer solution at pH=7.4.

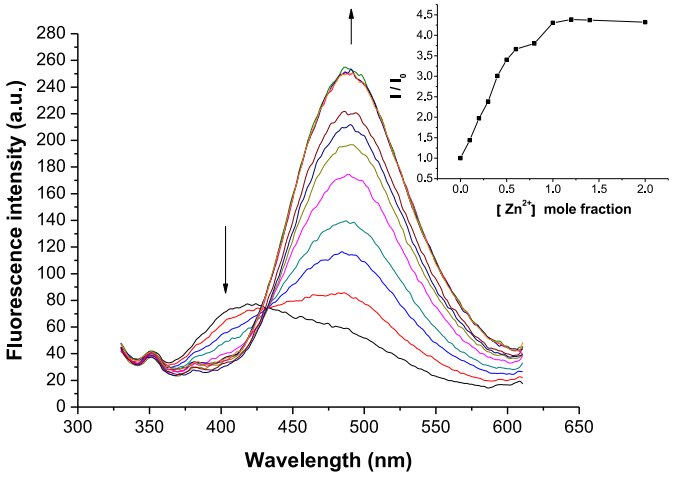

Fig. 2. Fluorescence spectra (λ_{ex}=316 nm) of **ACAQ** (5 μM) upon the titration of Zn^{2+} (0–2.0 equiv) in buffer solution (50 mM, HEPES, 50% methanol, pH=7.4). Inset: fluorescence intensity ratio as a function of Zn^{2+} concentration.

To define the application scope of the probe in metal sensing, 1 equiv of other metal ions was separately introduced into the probe. Fig. 3 shows that among biological relevant cations (i.e., Na^+, K^+, Ca^{2+}, and Mg^{2+}) and transition metals only Cd^{2+} can induce ratiometric fluorescence changes of the probe. It is a fairly common phenomenon that cross-interference caused by Cd^{2+} would affect

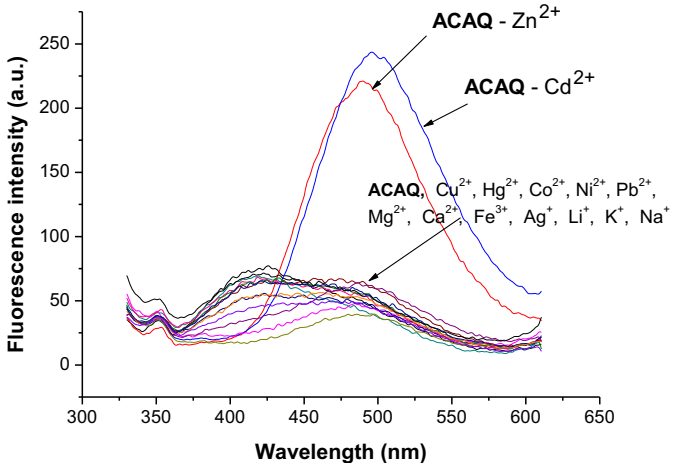

Fig. 3. Fluorescence emission spectra (λ_{ex}=316 nm) of **ACAQ** (5 μm) in the presence of various metal ions.

Zn^{2+} chemosensing.[5e,g] In addition, in consistent with the findings in UV–vis titration of the probe, Cu^{2+} exhibits quenching effect on the probe. To unravel the potential interference effect of Cd^{2+} and Cu^{2+} on the Zn^{2+} sensing probe, the corresponding binding constant of these three metal–**ACAQ** system was estimated from nonlinear fitting of the fluorescence titration curve and the results are compiled in Table 1, together with the values of binding constants obtained from UV–vis titration (vide supra).

Table 1
Association constants of Zn^{2+}, Cd^{2+}, and Cu^{2+} with the probe estimated by UV–vis and fluorescence titration method[a]

Metal–probe	K_a (UV–vis)	R^2 (linearity)	K_a (Fluor.)	R^2 (linearity)
Zn^{2+}–**ACAQ**	1.84×10^6	0.987	2.36×10^7	0.920
Cd^{2+}–**ACAQ**	3.20×10^6	0.993	1.78×10^8	0.998
Cu^{2+}–**ACAQ**	1.92×10^6	0.964	5.68×10^7	0.988

[a] Based on the titration of **ACAQ** (5 μM) in 50% HEPES pH 7.4 buffered methanol solution with metal perchlorate solutions.

The exact value of the binding constants obtained from two spectroscopic methods is quite different, but the relative magnitude of these constants is in good agreement. Owing to the higher sensitivity of the fluorescence method over the UV–vis method, we believe among common metal ions, **ACAQ** can form stable complex with all three metal ions (i.e., in nM level) as revealing by the strength of the respective association constant.

To evaluate the binding mode of **ACAQ**–Zn^{2+} complex, detailed ^{1}H NMR titration was carried out (Fig. 4). Upon gradual addition of Zn^{2+} to the CD_3OD-d_4/D_2O (8:2) solution of **ACAQ**, within the addition of 0.5 equiv of Zn^{2+}, a large downfield shift of H_1 ($\Delta\delta$=0.20) and H_3 ($\Delta\delta$=0.25), ascribed to the *ortho*-, *para*-aromatic protons to the quinoline nitrogen, was observed. The interaction between metal and quinoline nitrogen triggered the electron charge moving from the carboxamido group into the aromatic ring. As a result, a large upfield shift of the amide proton H_9 from δ 11.51 to 10.62 was observed. At the same time, the protons H_8 and H_{10} adjacent to the amine nitrogens also exhibited a large downfield shift ($\Delta\delta$=0.20) as a result of metal binding. Interestingly, upon continuous addition of Zn^{2+} to the sensing probe, no further change on the chemical shift of H_8 and H_{10} was observed. In contrast, further downfield shield of H_1 and H_3 was apparent. The observations suggested that within the addition of 0.5 equiv of Zn^{2+} both amine nitrogens and the quinolinyl nitrogen of **ACAQ** were heavily involved in the metal complexation. Further addition of Zn^{2+} only affected the quinoline ring protons and no effect on H_8 and H_{10} was evident. On the basis of the fact that Zn^{2+} has the propensity to attain a state of six coordination and the binding ability of amino group and that of quinolyl nitrogen is strong for Zinc metal, a two phase binding modes between Zn^{2+} and the probe is proposed (Fig. 5). According to the proposed model, when 0.5 equiv of Zn^{2+} was introduced into the sensor solution, the binding capacity of amino groups was fully satisfied and half of the quinolinyl nitrogen chelating capability was retained. When more Zn^{2+} was introduced, the carbonyl group of the amide moieties and the intact quinolinyl nitrogen of **ACAQ** provided binding sites to the metal. Thus, further downfield shift of H_1 and H_3 was observed and the chemical shift of amido-proton H_9 rebounded to δ 11.09. The chemical induced shift (CIS) of the specific protons of the probe as the function of [Zn^{2+}]/[**ACAQ**] (Fig. S4, Supplementary data) corroborated well with this binding mode. Importantly, all these observations suggested the direct interaction between the ligating groups of the probe and Zn^{2+} (Fig. 5).

Convincing evidence on the 1:1 binding mode of the complex of **ACAQ** and Zn^{2+} was obtained by the Job's plot (Fig. S5, Supplementary data) and the MALDI-TOF HRMS spectroscopic data. When the complex was subjected to mass spectral

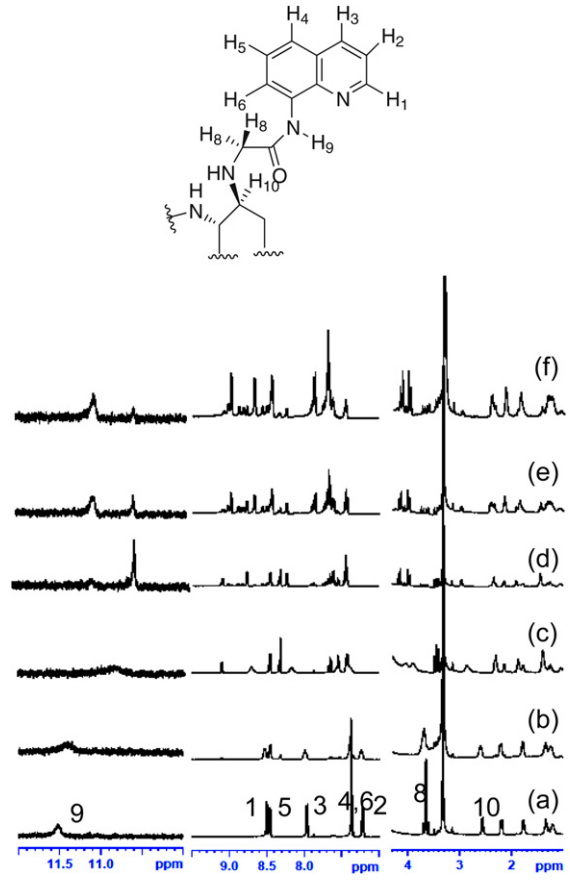

Fig. 4. Partial ^{1}H NMR spectra (400 MHz) of **ACAQ** (5 mM) in CD_3OD-d_4: D_2O (8:2) (a) free **ACAQ**; (b) **ACAQ**+0.1 equiv of Zn^{2+}; (c) **ACAQ**+0.3 equiv of Zn^{2+}; (d) **ACAQ**+0.5 equiv of Zn^{2+}; (e) **ACAQ**+0.8 equiv of Zn^{2+}, (f) **ACAQ**+1.0 equiv of Zn^{2+}.

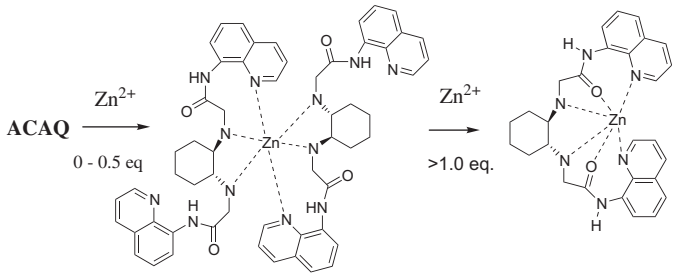

Fig. 5. Proposed binding modes of **ACAQ**–Zn^{2+} complex at two different stages.

measurement, a clear peak of *m*/*z* 545.1637 corresponding to $[M+Zn-H]^+$ was observed (Fig. S6, Supplementary data). On the basis of the combined spectroscopic information, the binding mode of **ACAQ**–Zn^{2+} is proposed in Fig. 5.

The selectivity of **ACAQ** to various metal ions was examined systematically. Only Zn^{2+} and Cd^{2+} can induce a dramatic ratiometric fluorescence enhancement of **ACAQ** and we are aware that the interference of Cd^{2+} was also observed for other zinc fluorescent sensors.[5a,e,g] On the other hand, Cu^{2+}, Fe^{3+}, and Co^{2+} quench the probe to different extent (Fig. 6). Particularly, Cu^{2+} emerged as an effective quencher for **ACAQ**. The probe did not respond properly with Zn^{2+} if weakly quenchers, such as Fe^{3+} and Co^{2+} are present in the solution prior to the addition of Zn^{2+}. Interestingly, if **ACAQ** was added into a mixture containing both Zn^{2+} and the potentially interfered ions (i.e., Cu^{2+}, Cd^{2+}, Fe^{3+}, Co^{2+}), as shown in Fig. 7, the presence of those foreign ions would not cause any interference effect on the fluorescence at 490 nm. The observed results could be ascribed to the combination of kinetic and thermodynamic factor of competitive binding between the probe and metal ions.

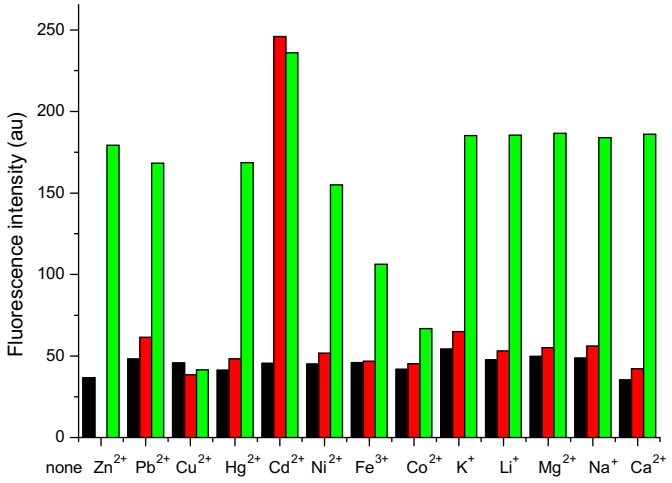

Fig. 6. Metal ion selectivity profiles of **ACAQ** (5 μM) in the presence of various metal ions in buffer solution (50 mM, HEPES, 50% methanol, pH=7.4): (a) (black bar) fluorescence intensity at 490 nm of **ACAQ** as the control; (b) (red bars) fluorescence intensity at 490 nm of the probe in interacting with 1 equiv of Pb^{2+}, Cu^{2+}, Hg^{2+}, Cd^{2+}, Ni^{2+}, Fe^{3+}, K^+,Li^+,Mg^{2+}, Na^+, Ca^{2+}; (c) (green bars) fluorescence intensity of **ACAQ** in the mixture containing separately 1 equiv of Hg^{2+}, Pb^{2+}, Ni^{2+}, Co^{2+}, Cd^{2+}, Cu^{2+}, Li^+; 300 equiv of Na^+, K^+; 100 equiv of Ca^{2+}, Mg^{2+} then adding of 1 equiv of Zn^{2+}.

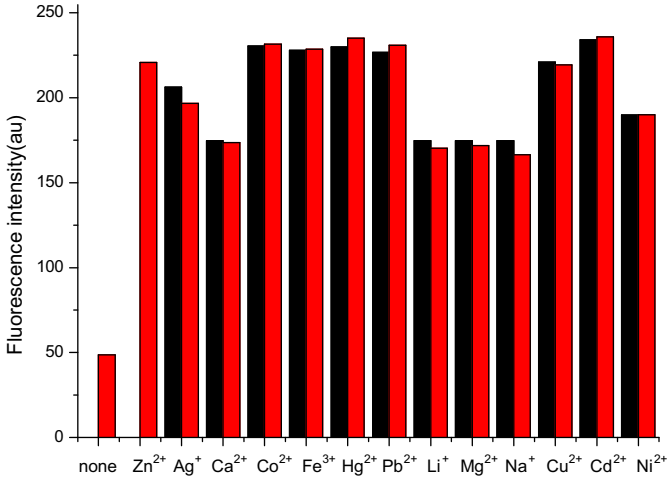

Fig. 7. Selectivity of **ACAQ** (5 μm) for Zn^{2+} in the presence of other metal ions in buffer solutions (50 mM, HEPES, 50% methanol, pH=7.4), λ_{ex}=316 nm. Red bars represent the fluorescence response of the probe to 1 equiv of Zn^{2+}; black bars show the subsequent addition of appropriate amount of potentially interfered metal ion (100 equiv for Li^+, Na^+, Ca^{2+}, Mg^{2+}, 1 equiv for all other metal ions) to the Zn^{2+}–**ACAQ** solution.

According to the relative stability of metal–**ACAQ** complex as shown in Table 1, it is quite unlikely that Cu^{2+} or Cd^{2+} can completely displace the Zn^{2+} from its **ACAQ** complex. The selectivity results reported in Fig. 7 corroborate well with this supposition. No fluorescence change of Zn^{2+}–**ACAQ** solution was observed when either 1 equiv of Cu^{2+} or Cd^{2+} solution was added into the complex. Careful competition studies revealed that the kinetic aspect of the cation-exchange became clear. Due to the relatively small size of Zn^{2+} in comparing with that of Cu^{2+} and Cd^{2+}, it should form a reasonably tight complex with **ACAQ**. Addition of 1 equiv of Cu^{2+} into the Zn^{2+}–**ACAQ** complex, no reduction of the emission peak at 490 nm was detected after 30 min, indicating that the displacement of Zn^{2+} from its tight complex by the larger Cu^{2+} ion is thermodynamically unfavorable, but also kinetically rather sluggish. As shown in Fig. 8,

increasing the amount of Cu^{2+} from 1 equiv to 3 equiv and then to 5 equiv separately, after 30 min in each of the cases, could only reduce the fluorescence of Zn^{2+}–**ACAQ** complex by 5% and 10%, respectively. On the other hand, adding 1 equiv of Zn^{2+} to the Cu^{2+}–**ACAQ** complex did not trigger any observable change in its fluorescence spectrum, which is in consistent with the comparable associate constants of Cu^{2+}, Zn^{2+}, and **ACAQ** (vide supra).

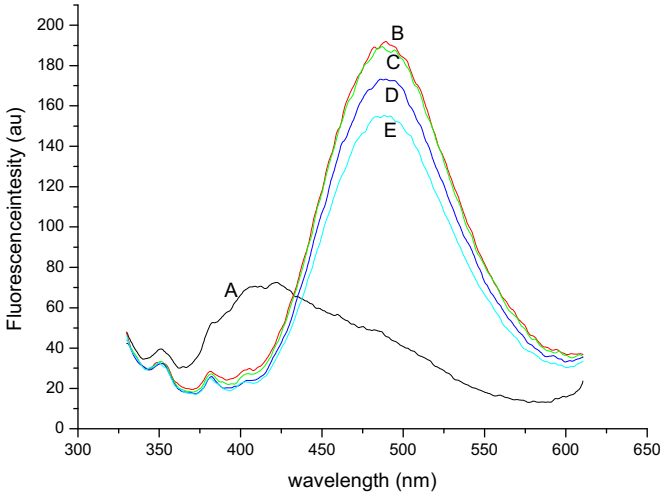

Fig. 8. Negligible quenching effect observable from the addition of 1, 3, 5 equiv of Cu^{2+} into Zn^{2+}–**ACAQ** (5 μM) in buffer solution after the time lag of 30 min (50 mM, HEPES, 50% methanol, pH=7.4). (A): 5 μM **ACAQ** in buffer solution (50 mM, HEPES, 50% methanol, pH=7.4); (B): (A)+1 equiv Zn^{2+}; (C): (B)+1 equiv Cu^{2+}, (D): (C)+2 equiv Cu^{2+}, (E): (D)+2 equiv Cu^{2+}.

In contrast, according to the quenching experiments performed on adding Cu^{2+} into the Cd^{2+}–**ACAQ** solution as shown in Fig. S7, Supplementary data, 1 equiv of Cu^{2+} is sufficient and effective to replace Cd^{2+} from its relative loose complex with **ACAQ**, resulting in the suppression of the emission peak at 490 nm.

To make room for developing analytical procedure for detecting Zn^{2+} in biological and environmental samples, the small but significant interference effect caused by Cu^{2+} and Cd^{2+} can be completely removed by using diethyldithiocarbamate as the screening agent.[11] For instance, the quenching effect caused by Cu^{2+} on Zn^{2+} detection can be completely eliminated by the use of 5 equiv of diethyldithiocarbamate (Fig. 9, curve C vs D). The enhanced

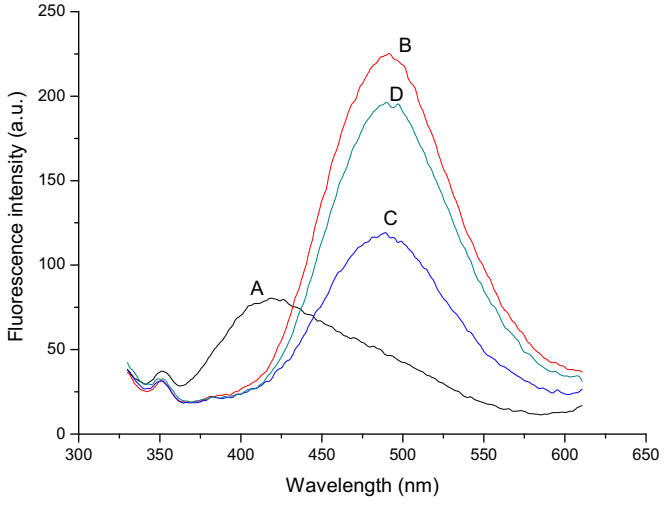

Fig. 9. Effect of masking agent diethyldithiocarbamate on the detection of a mixture of Cu^{2+} and Zn^{2+} by **ACAQ**—(A): 5 μM **ACAQ** in buffer solution (50 mM, HEPES, 50% methanol, pH=7.4); (B): (A)+1 equiv Zn^{2+}; (C): (B)+1 equiv Cu^{2+}; (D): (C)+5 equiv diethyldithiocarbamate.

fluorescence effect triggered by Cd^{2+} on Zn^{2+} determination is also removed completely by the action of the screening agent (Fig. S8, Supplementary data). Furthermore, to establish the reversibility of the binding of Zn^{2+} to **ACAQ**, the fluorescence enhancement of the probe at 490 nm triggered by 1 equiv of Zn^{2+} can be turn-off by the addition of 15 equiv of EDTA. The same extent of fluorescence enhancement can be recovered when an additional 17 equiv of Zn^{2+} was introduced (Fig. 10).

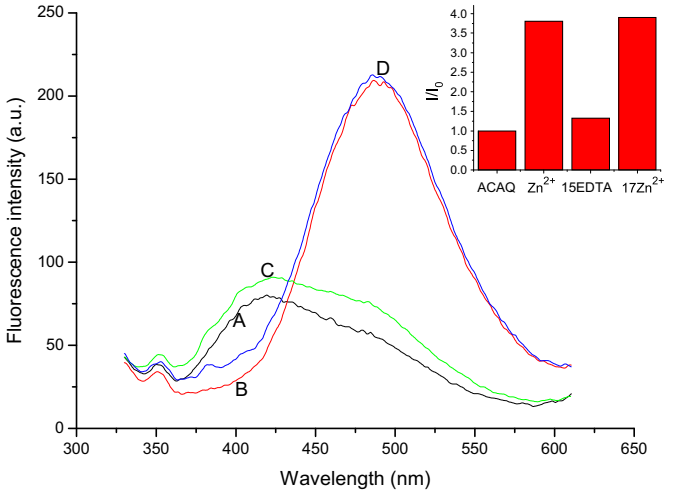

Fig. 10. Demonstration of the reversible binding of **ACAQ**–Zn^{2+} (A): 5 μM **ACAQ** in buffer solution (50 mM, HEPES, 50% methanol, pH=7.4); (B): (A)+1 equiv Zn^{2+}; (C): (B)+15 equiv EDTA; (D): (C)+17 equiv Zn^{2+} (inset: two cycles of reversible binding).

The rich fluorescence response characteristics of **ACAQ** toward various metal ions also provide opportunity for us to build up fluorescent switches.[12] The fluorescence of **ACAQ** at 490 nm upon excitation at 416 nm in aqueous methanolic buffer solution was enhanced upon addition of Zn^{2+}, then it was significantly quenched by the addition of 35 equiv of Fe^{3+}. The on-state can be re-established by adding 40 equiv of Zn^{2+}. Then, sequential titration of **ACAQ** by Fe^{3+} and Zn^{2+} caused the fluorescence to be quenched (OFF) and enhanced (ON) (Fig. 11).

To demonstrate the Zn-specific response of **ACAQ** in a cellular environment, the HK-1 cells were treated with **ACAQ** alone or **ACAQ**/Zn solution at 37 °C for 3 h. Untreated cells displayed negligible background fluorescence (Fig. 12a). A strong fluorescence

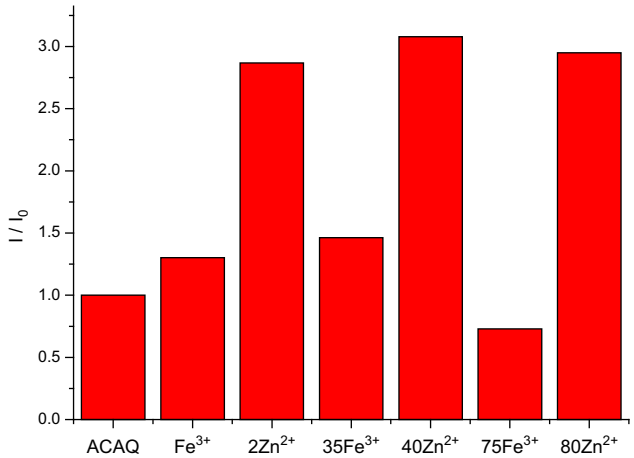

Fig. 11. Fluorescence output (I/I_0) at 490 nm of **ACAQ** in 1:1 aqueous methanolic pH 7.4 HEPES buffer solution upon alternate addition of Fe^{3+} and Zn^{2+} (1 equiv/2 equiv/35 equiv/40 equiv/75 equiv/80 equiv). λ_{ex}=316 nm.

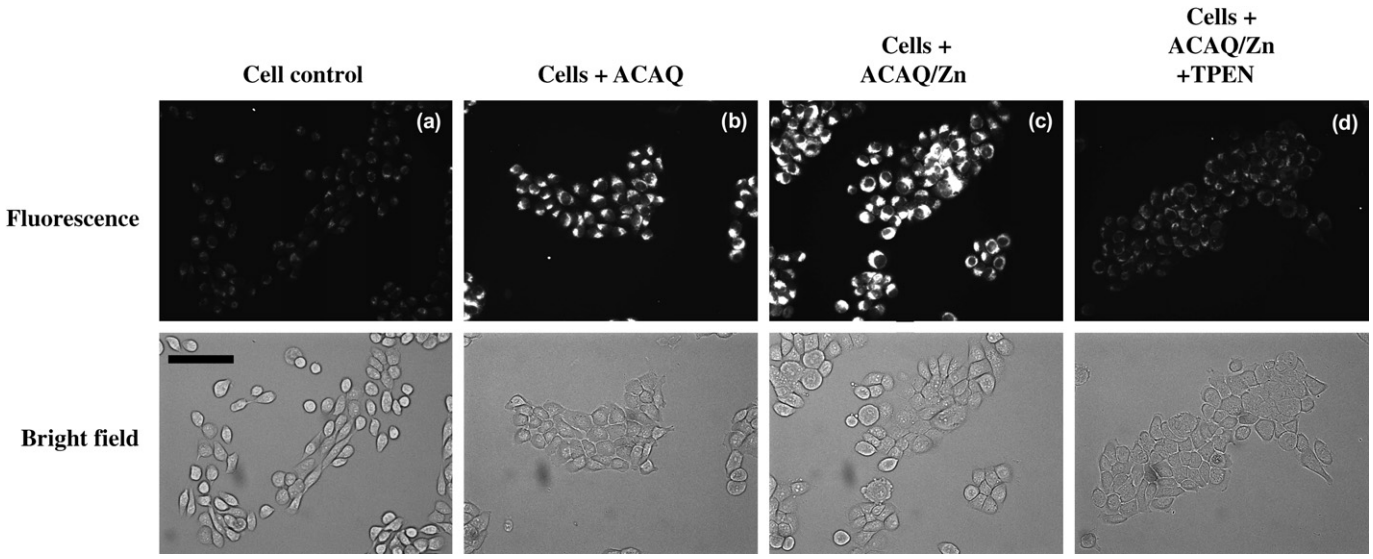

Fig. 12. Fluorescence imaging of **ACAQ** in HK-1 cells. HK-1 cells were untreated (a), incubated with **ACAQ** (b) or incubated with **ACAQ**/Zn solution (c). The cells were then incubated at 37 °C for 3 h before capturing of the images. The effect of metal chelator, TPEN, on the emission of **ACAQ**/Zn was studied by incubating the **ACAQ**/Zn-treated cells with TPEN at 37 °C for 1 h before capturing of the images (d). Scale bar: 100 μm.

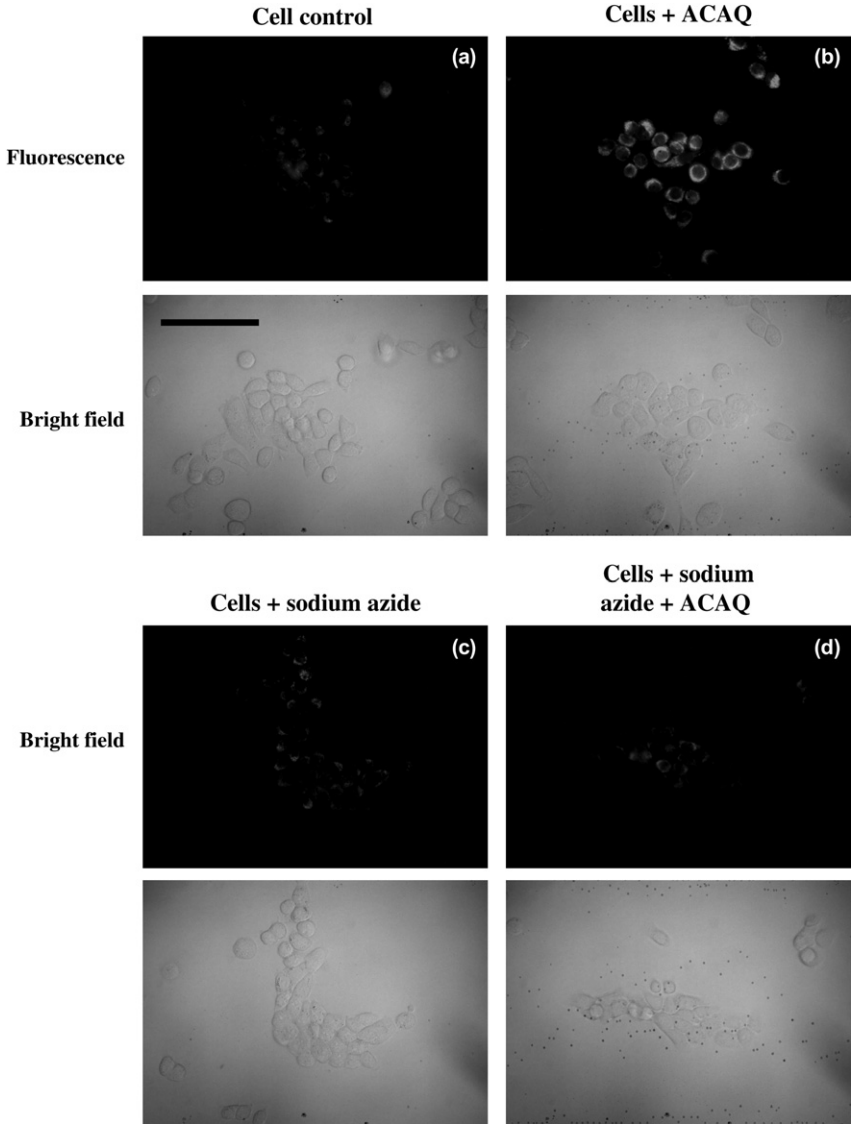

Fig. 13. Metabolic inhibition by sodium azide prevents cellular uptake of **ACAQ**. HK-1 cells were untreated (a and b) or pre-treated with sodium azide (10 mM) for 1 h (c and d) at 37 °C. The cells were then incubated with **ACAQ** for 3 h before capturing of the images. The cells were then washed and the emitted fluorescent signals of **ACAQ** were captured under a fluorescence microscope (Axioskop 2, Carl Zeiss) equipped with a mercury bulb and ultraviolet filters (excitation filter, G 365 nm; emission filter, LP 420 nm). Scale bar: 100 μm.

signal was observed in the cytoplasm of **ACAQ**-treated cells (Fig. 12b). Moreover, **ACAQ**/Zn-treated cells exhibited a stronger fluorescence signal (Fig. 12c) than the cells treated with **ACAQ** alone (Fig. 12b). In contrast, the fluorescence signal of **ACAQ**/Zn-treated cells was quenched by subsequent incubation with metal chelator, *N*,*N*,*N*′,*N*′-terakis(2-pyridylmethyl)ethylenediamine (TPEN) (Fig. 12d). The weak fluorescence images could be due to the fact that some of the **ACAQ**s were removed together with the TPEN bound Zn^{2+} from the cell. This finding indicated that the fluorescence emission was a result of reversible Zn binding to the **ACAQ** in the cell environment.

To further address the issue on the process of cellular uptake of **ACAQ**, HK-1 cells were pre-treated with sodium azide, an agent known to inhibit cellular respiration, for 1 h followed by co-incubation with **ACAQ** and sodium azide for 3 h. The background fluorescence of cells receiving sodium azide alone (Fig. 13c) was similar to the control cells (Fig. 13a). A strong fluorescence signal was observed in the cytoplasm of **ACAQ**-treated cells (Fig. 13b). However, the fluorescence signal in the cytoplasm of sodium azide-pre-treated cells (Fig. 13d) was similar to the control cells (Fig. 13a), indicating that the cellular uptake of **ACAQ** was abolished after metabolic inhibition.

3. Conclusions

By incorporating two 8-aminoquinoline moieties onto *trans*-1,2-diaminocyclohexene backbone with suitable spacers, a highly selective and sensitive fluorescent Zn^{2+} probe, **ACAQ**, was designed and constructed. Under physiological pH conditions, in vitro ratiometric detection of Zn^{2+} at subnanomolar concentration can be achieved in aqueous methanol solution. The rich metal binding characteristics of **ACAQ** permits us developing a molecular switch. Using fluorescent microscopic method, Zn^{2+} imaging of living cells by our probe has been realized. Furthermore, the cell permeation and imaging process of **ACAQ** was demonstrated by fluorescent microscopic method.

4. Experimental

4.1. General methods

The melting point was determined with a MEL-TEMPII melting point apparatus (uncorrected). ^{1}H NMR and ^{13}C NMR spectra were recorded on a VARIAN INOVA or Bruka Advance-III 400 spectrometer (at 400 and 100 MHz, respectively) in $CDCl_3$. Low resolution mass spectra were recorded on a Finnigan MAT SSQ-710 mass spectrometer while high resolution mass spectra were obtained on a Bruker Autoflex mass spectrometer (MALDI-TOF). Fluorescent emission spectra and UV–vis spectra were collected on a PE LS50B and a Cary UV-100 spectrometer, respectively. Unless specified, all fine chemicals were used as received.

4.2. Synthesis of ACAQ

To the chloroform solution (30 ml) of (1*R*, 2*R*)-cyclohexane-1,2-diamine(0.11 g, 1.0 mmol), 2-bromo-*N*-(quinolin-8-yl)acetamide (0.53 g, 2.0 mmol),[7b] and triethylamine (0.53 ml, 4.5 mmol) were introduced successively. The reaction mixture was stirred at rt for 6 h. Then water was added, and the mixture was extracted with $CHCl_3$ (3×20 ml), and the combined organic layers were dried over anhydrous sodium sulfate. After filtered, removal of the solvent in vacuo, the residue was purified by column chromatography on SiO_2 using DCM/MeOH=20:1 (v:v) as the eluant to afford **ACAQ** as white solids (0.29 g, 61% yield). Mp: 178 °C–180 °C. ^{1}H NMR (400 MHz, $CDCl_3$): 11.46 (2H, s), 8.71 (2H, dd, *J*=7.6, 1.2 Hz), 8.57 (2H, dd, *J*=4.2, 1.6 Hz), 7.89 (2H, dd, *J*=8.2, 1.6 Hz), 7.45–7.41 (2H, m), 7.35–7.32 (2H, m), 7.17 (2H, dd, *J*=8.2, 4.2 Hz), 3.67 (1H, d, *J*=4.0 Hz), 2.54–2.52(4H, m), 1.74–1.71 (2H, m), 1.26–1.23 (2H, m), 1.16–1.13 (2H, m); ^{13}C NMR (400 MHz, $CDCl_3$): 171.3, 148.3, 138.7, 135.7, 134.1, 127.8, 127.0, 121.5, 121.4, 116.2, 62.3, 51.3, 31.8, 24.8. HRMS (MALDI-TOF) *m*/*z* calcd for $C_{28}H_{30}N_6O_2$ $[M+1]^+$ 483.2503, found 483.2533.

4.3. Cell culture

Human nasopharyngeal carcinoma cells (HK-1)[13] were maintained in RPMI 1640 (Gibco) supplemented with 10% FBS (Gibco) and antibiotics (penicillin 50 U/ml; streptomycin 50 μg/ml). The cells were incubated at 37 °C in a humidified CO_2 (5%) incubator.

4.4. Fluorescence microscopic imaging of ACAQ

HK-1 cells (3×10^5 cells) were seeded onto coverslip in 35-mm culture dishes for overnight. **ACAQ** (10 μM) was mixed with zinc acetate (40 μM) in culture medium and incubated with the cells for 3 h in dark, the cells were then followed by incubation with TPEN (20 μM) for 1 h. The cells were then washed and the emitted fluorescent signals of **ACAQ** were captured under a fluorescence microscope (ECLIPSE T*i*, Nikon) equipped with a mercury bulb and ultraviolet filters (excitation filter, 325–375 nm; emission filter, 435–485 nm).

Acknowledgements

The work was supported by grant from the Research Grant Council of Hong Kong (HKBU 200208) and Hong Kong Baptist University (FRG1/10-11/026).

Supplementary data

Supplementary data contain UV titration curves of **ACAQ** and Cu^{2+}, Cd^{2+}, the dependence of fluorescence of **ACAQ** and its Zn^{2+} complex with pH, chemical induced shift of some selected proton resonates of **ACAQ** as the function of $[Zn^{2+}]$/[**ACAQ**], a Job's plot, HRMS of **ACAQ**–Zn^{2+}, quenching effect of Cu^{2+} on the fluorescence of **ACAQ**–Cd^{2+} complex, effect of masking agent on the detection of Cd^{2+} and Zn^{2+} mixture, HRMS, ^{1}H, ^{13}C NMR and ^{1}H–^{1}H COSY spectrum of **ACAQ**. Supplementary data associated with this article can be found in the online version at doi:10.1016/j.tet.2011.03.053.

References and notes

1. For reviews, see: (a) *Fluorescent Chemosensors for Ion and Molecular Recognition*; Czarnik, A. W., Ed.; American Chemical Society: Washington, DC, 1993; (b) de Silva, A. P.; Gunaratne, H. Q. N.; Gunnlaugsson, T.; Huxley, T. M.; McCoy, C. P.; Rademacher, J. T.; Rice, T. E. *Chem. Rev.* **1997**, *97*, 1515–1566; (c) Martinez-Manez, R.; Sancanon, F. *Chem. Rev.* **2003**, *103*, 4419–4476; (d) Gunnlaugsson, T.; Glynn, M.; Tocci, G. M.; Kruger, P. E.; Pfeffer, F. M. *Coord. Chem. Rev.* **2006**, *250*, 3094–3117.
2. Selected recent examples: (a) Burdette, S. C.; Walkup, G. K.; Spingler, B.; Tsien, R. Y.; Lippard, S. J. *J. Am. Chem. Soc.* **2001**, *123*, 7831–7841; (b) Jiang, P.; Chen, L.; Lin, J.; Liu, Q.; Ding, J.; Gao, X.; Guo, Z. *Chem. Commun.* **2002**, 1424–1425; (c) Ko, S.-K.; Yang, Y.-K.; Tae, J.; Shin, I. *J. Am. Chem. Soc.* **2006**, *128*, 14150–14155; (d) Taki, M.; Desaki, M.; Ojida, A.; Lyoshi, S.; Hirayma, T.; Hamachi, I.; Yamamoto, Y. *J. Am. Chem. Soc.* **2008**, *130*, 12564–12565; (e) Zhang, X.; Xiao, Y.; Qian, X. *Angew. Chem., Int. Ed.* **2008**, *47*, 8025–8029.
3. (a) Lippard, S. J.; Berg, J. M. *Principle of Bioinogranic Chemistry*; University Science Book: CA, 1994, pp 10, 14, 78–183; (b) Nolan, E. M.; Lippard, S. J. *Acc. Chem. Res.* **2009**, *42*, 193–203.
4. (a) Bush, A. I. *Curr. Opin. Chem. Biol.* **2000**, *4*, 184–191; (b) Cuajungco, M. P.; Faget, K. Y. *Brain Res. Rev.* **2003**, *41*, 44–56.
5. Selected recent examples: (a) Hanaoka, K.; Kikuchi, K.; Kojima, H.; Urano, Y.; Nagano, T. *J. Am. Chem. Soc.* **2004**, *126*, 12470–12476; (b) Royzen, M.; Durandin, A.; Young, V. G.; Geachintov, N. E.; Canary, J. W. *J. Am. Chem. Soc.* **2006**, *128*, 3854–3855; (c) Parkesh, R.; Lee, T. C.; Gunnlaugsson, T. *Org. Biomol. Chem.* **2007**, *5*, 310–317; (d) Liu, Y.; Zhang, N.; Chen, Y.; Wang, L.-H. *Org. Lett.* **2007**, *9*, 315–318; (e) Wang, H.-H.; Gan, Q.; Wang, X.-J.; Xue, L.; Liu, S.-H.; Jiang, H. *Org. Lett.* **2007**, *9*, 4995–5002; (f) Zhang, Y.; Guo, X.; Si, W.; Jia, L.; Qian, X. *Org. Lett.*

2008, *10*, 473–476; (g) Xue, L.; Liu, C.; Jiang, H. *Org. Lett.* **2009**, *11*, 1655–1658; (h) Wang, J.; Ha, C.-S. *Tetrahedron* **2009**, *65*, 6959–6964.
6. Xu, Z.; Baek, K.-H.; Kim, H. N.; Cui, J.; Qian, X.; Spring, D. R.; Shin, I.; Yoon, J. *J. Am. Chem. Soc.* **2010**, *132*, 601–610.
7. (a) Zhu, J.-F.; Yuan, H.; Chan, W.-H.; Lee, A. W. M. *Tetrahedron Lett.* **2010**, *51*, 3550–3554; (b) Zhu, J.-F.; Yuan, H.; Chan, W.-H.; Lee, A. W. M. *Org. Biomol. Chem.* **2010**, *8*, 3957–3964.
8. *Fluorescent Chemosensors for Ion and Molecule Recognition*; Czarnik, A. W., Ed.; American Chemical Society: Washington, DC, 1992.
9. Zhou, X.; Yu, B.; Guo, Y.; Tang, X.; Zhang, H.; Liu, W. *Inorg. Chem.* **2010**, *49*, 4002–4007.
10. (a) Rurack, K.; Kollmannsberger, M.; Resch-Genger, U.; Daub, J. *J. Am. Chem. Soc.* **2000**, *122*, 968–969; (b) Callan, J. F.; de Silva, A. P.; Ferguson, J.; Huxley, A. J. M.; O'Brien, A. M. *Tetrahedron* **2004**, *60*, 11125–11131; (c) Liu, Y.; Hau, H.; Zhang, H.-Y.; Yang, L.-X.; Jiang, W. *Org. Lett.* **2008**, *10*, 2873–2876.
11. *Dictionary of Analytical Reagents*; Townshend, A., Ed.; Chapman and Hall: New York, NY, 1993; pp 5656–5663.
12. (a) Kumar, M.; Kumar, R.; Bhalla, V. *Chem. Commun.* **2009**, 7384–7386; (b) Zhang, D.; Zhang, Q.; Su, J.; Tian, H. *Chem. Commun.* **2009**, 1700–1702; (c) Kim, S. H.; Kim, J. S.; Chang, S.-K. *Org. Lett.* **2006**, *8*, 371–374.
13. Huang, D. P.; Ho, J. H.; Poon, Y. F.; Chew, E. C.; Saw, D.; Lui, M.; Li, C. L.; Mak, L. S.; Lai, S. H.; Lau, W. H. *Int. J. Cancer* **1980**, *26*, 127–132.